UV ABSORPTION CROSS-SECTIONS OF THE MONOMER AND DIMER OF FORMIC ACID

D. L. SINGLETON, G. PARASKEVOPOULOS and R. S. IRWIN

Division of Chemistry, National Research Council of Canada, Ottawa, Ontario K1A 0R6 (Canada)

(Received June 28, 1986; in revised form September 6, 1986)

Summary

Absorption cross-sections of the monomer and dimer of formic acid vapor at 302 K have been determined at 1 nm intervals from 195 to 250 nm by non-linear least-squares analysis of the per cent transmission of 29 pressures of formic acid at each wavelength. The observed blue shift of the absorption maximum of the dimer with respect to the monomer and the lack of vibrational structure in the spectrum of the dimer are discussed in terms of the effect of hydrogen bonding on $n-\pi^*$ transitions.

1. Introduction

The longest-wavelength absorption band of formic acid, beginning at about 260 nm and peaking at about 210 nm, is characterized as an $n-\pi^*$ transition [1 - 3] with the band at immediately lower wavelengths being suggested as a $\pi-\pi^*$ transition [1, 3]. Gaseous formic acid consists of a mixture of monomer and dimer, the latter having a cyclic doubly hydrogen-bonded structure [4]. We have been investigating the gas phase photochemistry of formic acid at 222 nm in the $n-\pi^*$ transition, and have determined the quantum yield [5] of production of OH from and its subsequent reaction [6] with the monomer and the dimer. In the determination of quantum yields, the absorption cross-sections were required at this wavelength for the monomer and the dimer of formic acid. With the exception of spectra at three pressures with undefined contributions from the monomer and dimer given by Calvert and Pitts [2], and absorption cross-sections in the region 226 - 240 nm obtained by Ramsperger and Porter [7] 60 years ago from a limited set of data, there are no values of absorption cross-sections in the literature for this wavelength region which is of interest to photochemistry. Our preliminary measurements at 222 nm and a few other discrete wavelengths differed significantly from the values of Ramsperger and Porter and, in addition, indicated that the ratio of the cross-sections of the monomer and dimer changed significantly with wavelength. In order to validate our previous measurements of the cross-sections, we designed experiments to

0047-2670/87/$3.50

measure the cross-sections at 1 nm intervals over the wavelength range 195 - 250 nm by measuring the transmission of a large number of total pressures of formic acid at each wavelength, and treating the data by non-linear least squares. The absorption cross-sections should be useful in photochemical studies, especially since we have established that the quantum yield of OH is essentially unity for the monomer and near zero for the dimer of formic acid [5].

2. Experimental details

Spectra were obtained on a Varian Cary 210 spectrophotometer with Suprasil cells 10 cm long in the sample and reference beams. The sample cell was connected directly (glass blown) to a glass vacuum system, so that the cell could be evacuated and filled *in situ*. The pressure of formic acid was measured directly during the scans of the spectra with MKS (0 - 1000 Torr range) and Vacuum General (0 - 10 Torr range) capacitance manometers. A microcomputer interfaced with the spectrophotometer recorded the transmission readings at 1 nm intervals. The spectral bandwidth was set at 1 nm, although a few spectra were scanned at a bandwidth of 0.25 nm. The data were transferred to a VAX computer for further processing.

Formic acid (Aldrich, 98%) was degassed by freeze–pump–thaw cycles. Gas chromatographic analysis of the liquid on a column of Porapak T confirmed the presence of 2 mol.% water, which is present as a stabilizing agent. The presence of this amount of water is tolerable because the vapor above a solution of formic acid and water is significantly enriched in formic acid. For a 98 mol.% solution of formic acid, the vapor pressure of water is only about 0.1% that of formic acid, according to an interpolation of the data in ref. 8.

3. Results

Sample spectra of formic acid at resolutions of 0.25 nm and 1 nm are given in Fig. 1, which show the nature of the absorption band and the vibrational fine structure. For the determinations of the cross-sections, spectra were obtained at 302 K for 29 pressures of formic acid (0.5 - 22 Torr) at 1 nm intervals between 195 and 250 nm at a resolution of 1 nm. Because the sample and reference cells were not perfectly matched, it was necessary to calculate the ratio of the transmission spectra of formic acid to the transmission spectrum of the evacuated cell. Spectra of the evacuated cell were obtained after every four to seven formic acid spectra, and the pairs of evacuated cell spectra bracketing a series of formic acid spectra were averaged and used to obtain the ratios for the bracketed spectra. The 29 ratioed data sets (corresponding to 29 pressures) were each composed of 56 transmission readings (corresponding to 56 different wavelengths). These

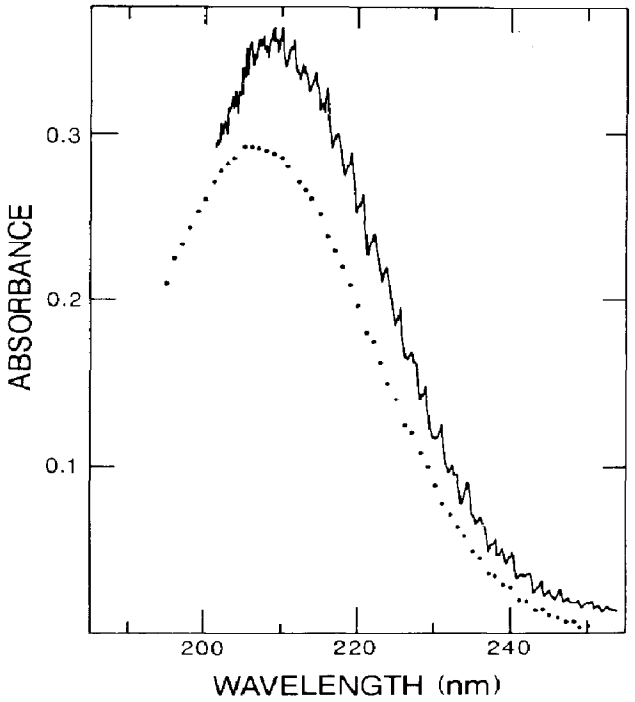

Fig. 1. Examples of spectra of formic acid: ——, 0.25 nm resolution, 10 Torr; ·····, 1.0 nm resolution, 8 Torr. Absorbance = $\log(I_0/I)$. The spectrum at 0.25 nm resolution has not been corrected for the absorbance of the evacuated cell. The cross-sections were determined with a resolution of 1 nm.

data sets were reorganized to give 56 data sets (corresponding to 56 different wavelengths) of 29 transmission readings (corresponding to each pressure). Each of the 56 data sets was used in a non-linear least-squares routine, which used Marquardt's algorithm [9, 10], to fit the cross-sections σ_M and σ_D of the monomer and dimer to the equation

$$\frac{I}{I_0} = \exp\{-l(\sigma_M[\text{monomer}] + \sigma_D[\text{dimer}])\} \quad (1)$$

at each wavelength (l is the length of the absorption cell).

Beer's law was found to be valid to within about 10% in an experiment at 222 nm (KrCl laser) in which the optical path length was varied from 10 to 89 cm for 5 Torr formic acid, corresponding to 76% - 10% transmission. The partial pressures of monomer and dimer were calculated from the equilibrium constant

$$K = \frac{[\text{monomer}]^2}{[\text{dimer}]} = 1.07 \times 10^{17} \text{ molecules cm}^{-3}$$

at 302 K taken from Halford's analysis [11] of vapor densities reported by Coolidge [12]. This value of K is in good agreement with the values extrapolated from higher temperatures from the work of Barton and Hsu [13] and of Büttner and Maurer [14] which are within +15% and —8% respectively of Halford's value.

Examples at several wavelengths of the transmission as a function of pressure of formic acid, together with the lines calculated from eqn. (1) using the fitted values of σ_M and σ_D, are given in Fig. 2. The values of σ_M and σ_D between 195 and 250 nm are given in Table 1 and plotted in Fig. 3.

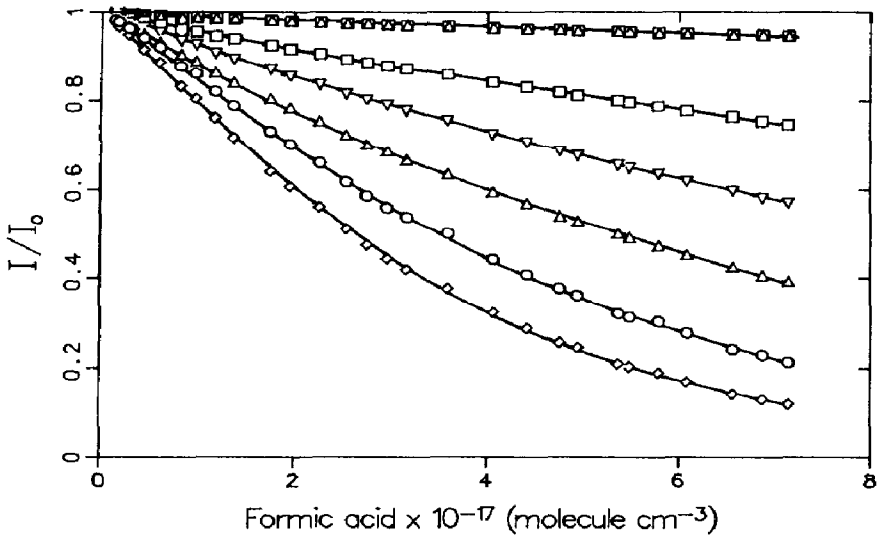

Fig. 2. Examples of transmission as a function of total pressure of formic acid at several wavelengths (○, 195 nm; ◇, 205 nm; △, 225 nm; ▽, 230 nm; ⊠, 235 nm; □, 245 nm). The lines are the non-linear least-squares fits of eqn. (1).

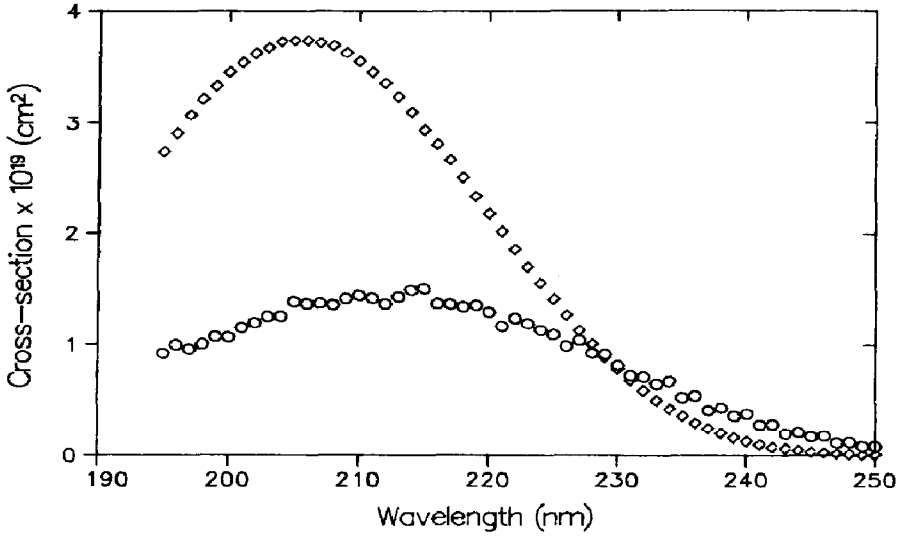

Fig. 3. Absorption cross-sections of the monomer (○) and dimer (◇) of formic acid as a function of wavelength.

TABLE 1

Absorption cross-sections for the monomer (σ_M) and dimer (σ_D) of formic acid[a]

Wavelength (nm)	σ_M ($\times 10^{-19}$ cm^2)	σ_D ($\times 10^{-19}$ cm^2)
250	0.0861 ± 0.0024	0.0072 ± 0.0014
249	0.0855 ± 0.0021	0.0093 ± 0.0012
248	0.123 ± 0.003	0.0134 ± 0.0017
247	0.118 ± 0.003	0.0190 ± 0.0015
246	0.179 ± 0.003	0.0267 ± 0.0017
245	0.173 ± 0.003	0.0337 ± 0.0015
244	0.210 ± 0.004	0.0490 ± 0.0022
243	0.198 ± 0.004	0.0659 ± 0.0022
242	0.283 ± 0.004	0.0795 ± 0.0026
241	0.279 ± 0.005	0.102 ± 0.003
240	0.379 ± 0.004	0.131 ± 0.003
239	0.358 ± 0.004	0.163 ± 0.002
238	0.432 ± 0.005	0.203 ± 0.003
237	0.410 ± 0.005	0.246 ± 0.003
236	0.540 ± 0.006	0.295 ± 0.003
235	0.524 ± 0.006	0.358 ± 0.004
234	0.668 ± 0.006	0.426 ± 0.004
233	0.644 ± 0.007	0.501 ± 0.004
232	0.707 ± 0.006	0.587 ± 0.004
231	0.718 ± 0.008	0.677 ± 0.005
230	0.812 ± 0.009	0.778 ± 0.005
229	0.915 ± 0.010	0.887 ± 0.006
228	0.924 ± 0.012	1.01 ± 0.01
227	1.04 ± 0.01	1.13 ± 0.01
226	0.987 ± 0.009	1.27 ± 0.01
225	1.09 ± 0.01	1.41 ± 0.01
224	1.13 ± 0.02	1.55 ± 0.01
223	1.19 ± 0.02	1.70 ± 0.01
222	1.24 ± 0.02	1.86 ± 0.01
221	1.16 ± 0.02	2.02 ± 0.01
220	1.29 ± 0.02	2.18 ± 0.01
219	1.35 ± 0.03	2.34 ± 0.02
218	1.34 ± 0.03	2.51 ± 0.02
217	1.36 ± 0.03	2.67 ± 0.02
216	1.37 ± 0.02	2.81 ± 0.02
215	1.50 ± 0.02	2.94 ± 0.01
214	1.49 ± 0.03	3.10 ± 0.02
213	1.43 ± 0.03	3.24 ± 0.03
212	1.36 ± 0.03	3.36 ± 0.03
211	1.42 ± 0.04	3.46 ± 0.03
210	1.44 ± 0.04	3.55 ± 0.03
209	1.41 ± 0.04	3.62 ± 0.03
208	1.36 ± 0.04	3.69 ± 0.03
207	1.37 ± 0.04	3.72 ± 0.03
206	1.36 ± 0.04	3.74 ± 0.03
205	1.38 ± 0.03	3.74 ± 0.03
204	1.25 ± 0.04	3.73 ± 0.03
203	1.25 ± 0.04	3.67 ± 0.03
202	1.19 ± 0.04	3.62 ± 0.03
201	1.15 ± 0.04	3.54 ± 0.03
200	1.07 ± 0.04	3.46 ± 0.03
199	1.07 ± 0.04	3.33 ± 0.03
198	1.00 ± 0.04	3.22 ± 0.03
197	0.957 ± 0.037	3.08 ± 0.03
196	0.996 ± 0.036	2.91 ± 0.03
195	0.918 ± 0.037	2.74 ± 0.03

[a]Indicated uncertainties are one standard deviation.

4. Discussion

The accuracy of the fitted values of σ_M and σ_D is expected to be poorer at the extremes of the wavelength range. At long wavelengths near the onset of absorption, the transmission is in the range 97% - 99%, even for higher pressures of formic acid. At the shortest wavelengths near 195 nm, the intensity of the lamp decreases, resulting in increasing noise levels. This is evident in the increasing fractional standard deviations at the extreme wavelengths, 3% and 20% for σ_M and σ_D at 250 nm and 4% and 1% at 195 nm, compared with the minima of 0.8% and 0.5% at 227 nm.

The choice of the monomer–dimer equilibrium constant K influences the fitted values of the absorption cross-sections. As mentioned earlier, the extrapolated results of more recent determinations of K are within +15% and —8% of the value adopted for our analysis, and we assume that the maximum uncertainty in our adopted value of K is probably less than 25%. The maximum uncertainty in σ_M and σ_D resulting from a ±25% variation in the value of K, determined at selected wavelengths, is as follows for σ_M and σ_D respectively: 195 nm, 13% and 2%; 210 nm, 10% and 2%; 222 nm, 4% and 0.8%; 250 nm, 5% and 27%. The influence of the value of K is seen to be greatest at the extremes of the wavelength range, and for the species with the lower absorption cross-section.

The results at 222 nm are 1.24×10^{-19} cm^2 and 1.86×10^{-19} cm^2 for σ_M and σ_D respectively, which compare well with the values $(1.31 \pm 0.10) \times 10^{-19}$ cm^2 and $(1.99 \pm 0.06) \times 10^{-19}$ cm^2 determined in our earlier work with a KrCl excimer laser (222 nm) [5], considering that the laser line is not exactly 222 nm and that its width was not determined. The results are also in agreement with a non-linear least-squares analysis of the absorbance at 222 nm at three pressures taken from Fig. 5-6 of ref. 2, which gives $\sigma_M = (0.74 \pm 0.37) \times 10^{-19}$ cm^2 and $\sigma_D = (1.89 \pm 0.18) \times 10^{-19}$ cm^2. However, the values at 228 nm in Table 1, $\sigma_M = 0.924 \times 10^{-19}$ cm^2 and $\sigma_D = 1.01 \times 10^{-19}$ cm^2, are significantly larger than those reported by Ramsperger and Porter [7], 0.11×10^{-19} cm^2 and 0.50×10^{-19} cm^2, determined at 313 K. The latter values were obtained, however, with very few data points and by a less direct analysis of the data.

Differences in the photochemistry of the monomer and dimer of formic acid have been observed by us, notably that the dimer does not produce free OH radicals, in contrast to the monomer for which the quantum yield is unity [5]. As well, several differences in the cross-sections of the monomer and dimer are evident in Fig. 3. The maximum value of σ_M occurs at wavelengths longer than that of σ_D, with the band for the monomer much broader and less peaked than that of the dimer. Also, the onset of the transition occurs at shorter wavelengths for the dimer than for the monomer. A similar effect has been reported for acetic acid [15]. The blue shift of the absorption by the dimer with respect to the monomer is consistent with the behavior of n–π^* transitions. The blue shift of n–π^* transitions on going from the gas phase to solutions in which the solvent can hydrogen bond with

the substrate has been interpreted as stabilization of the non-bonding orbital of the ground state by hydrogen bonding. In the $n-\pi^*$ excited state, there is one less electron in the non-bonding orbital, so that the hydrogen bond is weakened [16 - 18]. Theoretical calculations of Iwata and Morokuma [19] confirm these earlier considerations, and indicate that the hydrogen-bonding energy (per hydrogen bond) is about 5.5 kcal mol^{-1} less in the $n-\pi^*$ excited state than in the ground state (both in the planar configuration). Thus, in the gas phase, the greater stabilization of the non-bonding orbital of the carbonyl group in the hydrogen-bonded dimer results in a greater energy separation between the ground and excited states relative to the monomer. A value of the hydrogen-bond energy could be obtained from the 0,0 transitions of the monomer and dimer (not from the absorption maxima) [17]. However, the onset of absorption is difficult to determine, as the onset is not abrupt, with weak absorption by the monomer being detected even beyond 260 nm [1].

Despite the low spectral resolution, there is some evidence of more fine structure in σ_M than in σ_D, which appears to be greater than the expected random deviations as judged by the absence of any trace of structure in the curve for σ_D and by the magnitude of the standard deviations in Table 1. The fine structure has been assigned [1] to excitation of the carbonyl stretch (1080 cm^{-1}) and the OCO bending mode (400 cm^{-1}). In the spectrum obtained at 0.25 nm resolution, we have been able to identify most members of five of the seven progressions of the carbonyl stretch reported by Ng and Bell [1], the remaining members probably requiring greater resolution and greater path length to be observable. The lack of vibrational structure in the cross-section of the dimer has been indicated previously for formic acid [20] and fluoroacetic acid [21]. The washing out of vibrational structure in the dimer may be due to transitions to a greater number of low frequency vibrational modes of the dimer, or perhaps due to a shortened lifetime of the excited $n-\pi^*$ state of the dimer caused by crossing to a (calculated) slightly lower ^1B_g state [19]. In solution, hydrogen-bonding solvents remove the vibrational fine structure of $n-\pi^*$ transitions of solutes. This phenomenon has been attributed to the shortened lifetime of the excited $n-\pi^*$ state, which is a consequence of the unstable local geometry for hydrogen bonding in the initially formed excited state and rapid reorganization to a more stable structure [22]. Such an effect may be less important in the gas phase because of the slower rate of collision-induced vibrational relaxation.

The ratio σ_D/σ_M is greater than 1 for wavelengths greater than 229 nm, and the ratio of the values at the peak absorption for the dimer and for the monomer is 2.5, in close agreement with the value of 2 expected from the simple consideration of two monomer units in the dimer, and neglecting any influence of hydrogen bonding on the transition moment. (In contrast, Briegleb and Strohmeier [15] report that the maximum cross-section for the monomer of acetic acid is slightly larger than that of the dimer.) The ratio σ_D/σ_M varies with wavelength, and below 229 nm it is less than 1, reaching a minimum value over the range of measurements of 0.08 at 250 nm. This

is just a consequence of the blue shift of the dimer, and implies that the onset of absorption is at longer wavelengths for the monomer than the dimer.

Acknowledgment

We thank Dr. D. J. Worsfold for providing the spectrophotometer and data acquisition system. This is NRCC Paper No. 26150.

References

1 T. L. Ng and S. Bell, *J. Mol. Spectrosc., 50* (1974) 166.
2 J. G. Calvert and J. N. Pitts, Jr., *Photochemistry*, Wiley, New York, 1966, p. 428.
3 E. E. Barnes and W. T. Simpson, *J. Chem. Phys., 39* (1963) 670.
4 A. Almenningen, O. Bastiansen and T. Motzfeldt, *Acta Chem. Scand., 23* (1969) 2848.
5 G. S. Jolly, G. Paraskevopoulos and D. L. Singleton, to be submitted.
6 G. S. Jolly, D. J. McKenney, D. L. Singleton, G. Paraskevopoulos and A. R. Bossard, *J. Phys. Chem., 90* (1986) 6557.
7 H. C. Ramsperger and C. W. Porter, *J. Am. Chem. Soc., 48* (1926) 1267.
8 J. Timmermans, *The Physico-chemical Constants of Binary Systems in Concentrated Solutions*, Vol. 4, Wiley-Interscience, New York, 1960, p. 347.
9 D. W. Marquardt, *J. Soc. Ind. Appl. Math., 11* (1963) 431.
10 P. R. Bevington, *Data Reduction and Error Analysis for the Physical Sciences*, McGraw-Hill, New York, 1969, p. 235.
11 J. O. Halford, *J. Chem. Phys., 10* (1942) 582.
12 A. S. Coolidge, *J. Am. Chem. Soc., 50* (1928) 2166.
13 J. R. Barton and C. C. Hsu, *J. Chem. Eng. Data, 14* (1969) 184.
14 R. Büttner and G. Maurer, *Ber. Bunsenges. Phys. Chem., 87* (1983) 877.
15 G. Briegleb and W. Strohmeier, *Naturwissenschaften, 33* (1946) 344.
16 G. J. Brealey and M. Kasha, *J. Am. Chem. Soc., 77* (1955) 4462.
17 G. C. Pimentel, *J. Am. Chem. Soc., 79* (1957) 3323.
18 M. Ito, K. Inuzuka and S. Imanishi, *J. Chem. Phys., 31* (1959) 1694.
19 S. Iwata and K. Morokuma, *Theor. Chim. Acta, 44* (1977) 323.
20 E. Gorin and H. S. Taylor, *J. Am. Chem. Soc., 56* (1934) 2042.
21 H. Basch, M. B. Robin and N. A. Kuebler, *J. Chem. Phys., 49* (1968) 5007.
22 N. S. Bayliss and E. G. McRae, *J. Chem. Phys., 58* (1954) 1002.